Optica Applicata, Vol. XXXVII, No. 4, 2007

Propagation of polarized light through optical nanosuperlattices

KAROL TARNOWSKI, WŁODZIMIERZ SALEJDA, MICHAŁ H. TYC

Institute of Physics, Wrocław University of Technology, Wybrzeże Wyspiańskiego 27, 50-370 Wrocław, Poland

We investigate numerically transmittance of polarized electromagnetic wave through periodic and aperiodic binary multilayered nanostructures made of left- and right-handed materials. The transmittance is calculated as a function of light wavelength and incidence angle as well as ordering, refractive indices and thicknesses of superlattice layers. Thanks to extension of the transfer matrix formalism over the case of complex refraction angles, such effects as tunnelling, absorption and strong dispersion in left-handed metamaterials are taken into account. We find that these effects cannot be neglected and cause new transmission bands to appear in the areas where total internal reflection in a single metamaterial layer occurs.

Keywords: metamaterials, left-handed materials, superlattices.

1. Introduction

Recently, the wave transmission properties of: (1) spatially ordered systems [1–3], also with defined type of randomness [4], and (2) random systems [5–9], were the subject of intensive studies. In papers [10–16], we have developed and applied transfer matrix formalism which allows for computing transmittance, reflectance and absorption of polarized electromagnetic waves in any multilayered system, the layers of which are arranged by defined spatial order (*i.e.*, periodic, Fibonaccian and non-Fibonaccian superlattices). The random quasi-one-dimensional structures require a completely different approach for studying properties of light propagation.

Recent advances in the field of negative refraction metamaterials [17, 18] (so-called left-handed materials, LHM) give hopes for fabrication of structures exhibiting novel properties in the visible light range. We have focused our attention on binary systems (*i.e.*, containing two types of layers, denoted as A and B). The main purpose of our study is to investigate the properties of multilayered systems containing very thin slabs of LHMs and RHMs (right-handed materials). In such superlattices light tunneling can be observed.

2. The model of dispersion and absorption in metamaterials

We apply an approximation of homogeneous metamaterial. The optical properties of metamaterial layers are determined by their relative permittivity ε_r and permeability μ_r. The frequency dependences of both are given by the following Lorentz formulas:

$$\varepsilon_r(\omega) = 1 + \frac{\omega_{pe}^2}{\omega_{0e}^2 - \omega^2 - i\gamma_e\omega}$$
$$\mu_r(\omega) = 1 + \frac{\omega_{pm}^2}{\omega_{0m}^2 - \omega^2 - i\gamma_m\omega} \tag{1}$$

The applied formalism allows calculation to be performed in the case of $\omega_{pe} \neq \omega_{pm}$ and $\omega_{0e} \neq \omega_{0m}$. For simplicity, we have assumed $\omega_{pe} = \omega_{pm} = \omega_p$, $\omega_{0e} = \omega_{0m} = \omega_0$ and $\gamma_m = \gamma_e = \gamma$. As a result, $\varepsilon_r(\omega) = \mu_r(\omega)$, and there is no difference between s and p polarizations. The refractive index is determined by the formula

$$n(\omega) = \left[\varepsilon_r(\omega)\mu_r(\omega)\right]^{1/2}$$

In our calculations, we have assumed the following values of dispersion parameters [18]: resonant frequency $\omega_p = 2.22\times10^{15}$ Hz was set in the middle of the optical range ($\lambda = 550$ nm) in order to give $\mathrm{Re}(n) = -1$ for $\lambda = 500$ nm, and γ was taken as $10^{-3}\omega_p$. The dispersion curve obtained is presented in Fig. 1.

3. The characteristic matrix approach

The binary multilayered systems under study (Fig. 2) are composed of J isotropic and homogeneous layers with refractive indices n_j determined by their relative permittivities μ_j, permeabilities ε_j and thicknesses d_j, where the index j denotes the j-th layer and takes values from 0 to $J + 1$ ($j = 0$ for the external medium "in" and $j = J + 1$ for the external medium "out"). In a binary system, only two values of refractive index (n_A, n_B) and thickness (d_A, d_B) are possible.

The propagation of plane electromagnetic wave is investigated using the matrix formulation [10–16, 19]. The parameters are: wavelength λ, polarization (s or p), and incidence angle θ. This formulation relates the amplitudes of electric field vector of incident (E_{in}^+), transmitted (E_{out}^+) and reflected (E_{in}^-) waves.

$$\left[E_{\mathrm{in}}^+, E_{\mathrm{in}}^-\right]^T = \mathbf{D}_{\mathrm{in},1}\mathbf{P}_1\mathbf{D}_{1,2}\dots\mathbf{P}_J\mathbf{D}_{J,\mathrm{out}}\left[E_{J+1}^+, E_{J+1}^-\right]^T = \mathbf{\Gamma}\left[E_{J+1}^+, E_{J+1}^-\right]^T \tag{2}$$

where $E_{\mathrm{out}}^- = 0$, and Γ is the 2×2 characteristic matrix of the layered system. The propagation matrices $\mathbf{P}_j$ are diagonal, $(\mathbf{P}_j)_{11} = (\mathbf{P}_j)_{22}^* = \exp(i\phi_j)$, where

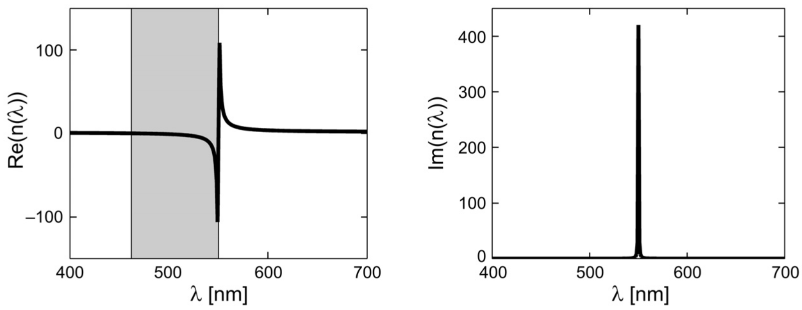

Fig. 1. Real and imaginary parts of refractive index assumed for LHM in calculations. Wavelength range where $\mathrm{Re}(n) < 0$ is marked in grey.

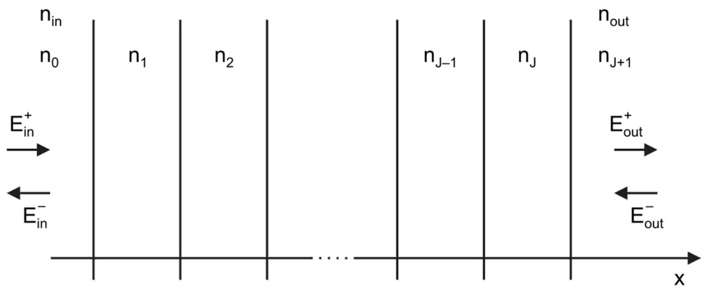

Fig. 2. Multilayered structure under study (for description, see the text).

$\phi_j = d_j n_j (2\pi/\lambda)\cos\theta_j$. The matrix $\mathbf{D}_{j,\,j+1}$, called the transmission matrix from the j-th to the $(j + 1)$-th medium, takes the form:

$$(\mathbf{D}_{j,\,j+1})_{11} = (\mathbf{D}_{j,\,j+1})_{22} = \frac{1}{t_{j,\,j+1}}$$

$$(\mathbf{D}_{j,\,j+1})_{12} = (\mathbf{D}_{j,\,j+1})_{21} = \frac{r_{j,\,j+1}}{t_{j,\,j+1}}$$

where the Fresnel coefficients of transmission $t_{j,\,j+1}$ and reflection $r_{j,\,j+1}$ for s and p waves are

$$t^s_{j,\,j+1} = \frac{2}{1 + \dfrac{\cos\theta_{j+1}}{\cos\theta_j}\left(\dfrac{\varepsilon_{j+1}\mu_j}{\varepsilon_j\mu_{j+1}}\right)^{1/2}}$$

$$t^p_{j,\,j+1} = \frac{2}{\dfrac{\cos\theta_{j+1}}{\cos\theta_j} + \left(\dfrac{\varepsilon_{j+1}\mu_j}{\varepsilon_j\mu_{j+1}}\right)^{1/2}}$$

$$r^s_{j,j+1} = \frac{1 - \dfrac{\cos\theta_{j+1}}{\cos\theta_j}\left(\dfrac{\varepsilon_{j+1}\mu_j}{\varepsilon_j\mu_{j+1}}\right)^{1/2}}{1 + \dfrac{\cos\theta_{j+1}}{\cos\theta_j}\left(\dfrac{\varepsilon_{j+1}\mu_j}{\varepsilon_j\mu_{j+1}}\right)^{1/2}}$$

$$r^p_{j,j+1} = \frac{\dfrac{\cos\theta_{j+1}}{\cos\theta_j} - \left(\dfrac{\varepsilon_{j+1}\mu_j}{\varepsilon_j\mu_{j+1}}\right)^{1/2}}{\dfrac{\cos\theta_{j+1}}{\cos\theta_j} + \left(\dfrac{\varepsilon_{j+1}\mu_j}{\varepsilon_j\mu_{j+1}}\right)^{1/2}}$$

in our case, $\left[(\varepsilon_{j+1}\mu_j)/(\varepsilon_j\mu_{j+1})\right]^{1/2} = 1$ and the coefficients for both polarizations are identical.

The transmittance T and reflectance R of the whole structure can be expressed in terms of elements of characteristic matrix:

$$T = \left|\frac{1}{\Gamma_{11}}\right|^2 \det\mathbf{\Gamma}$$

$$R = \left|\frac{\Gamma_{21}}{\Gamma_{11}}\right|^2$$

where $\mathbf{\Gamma}$ is computed by multiplying the propagation and transmission matrices of the system, as defined in Eq. (2). In the case of lossless layers, transmittance and reflectance sum up to one, otherwise absorption can be expressed as $A = 1 - (T + R)$.

4. Results

Transmittance, reflectance and absorption are calculated numerically and presented in greyscale maps. In all the maps, black points correspond to a value of zero and white points to one.

Single LHM layer. In the first step of our investigation, we have calculated transmitting properties of single LHM layer. Dispersion is given by Eq. (1). The layer is placed in air and its thickness $d = 40$ nm (Fig. 3) and $d = 1000$ nm (Fig. 4). Wavelength λ varies from 400 nm to 700 nm and incidence angle θ ranges from 0 to $\pi/2$.

Effect of the ordering of layers for selected binary superlattices. We have investigated different multilayered superlattices. In this paper, we focus on periodic

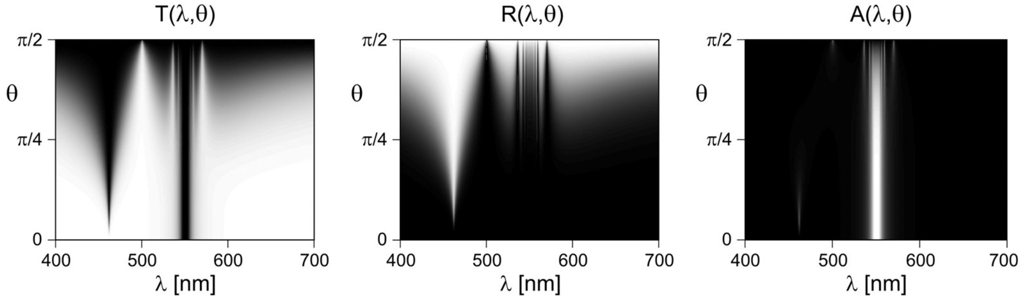

Fig. 3. Transmittance, reflectance and absorption for a single LHM nanolayer (d = 40 nm) placed in air.

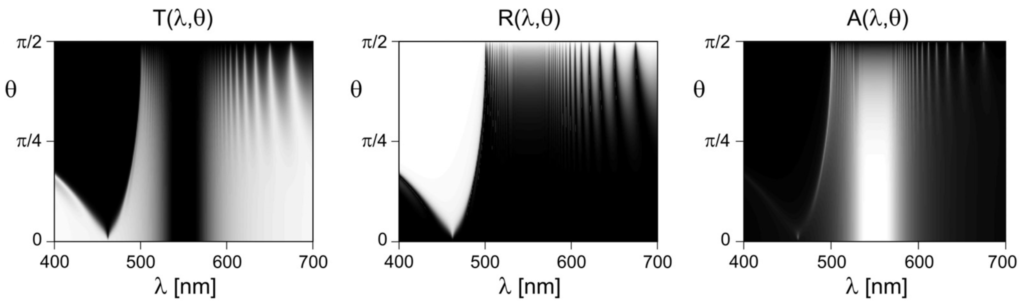

Fig. 4. Transmittance, reflectance and absorption for a single thick LHM layer (d = 1000 nm) placed in air.

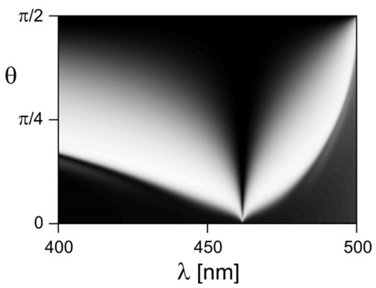

Fig. 5. Difference between transmittances for thin (d = 40 nm) and thick (d = 1000 nm) single metamaterial layers. The effect of tunneling appears.

(Fig. 5) and Fibonaccian (Fig. 6) structures. The parameters of superlattices include: the number of periods for periodic structures, and generation number for Fibonaccian ones. For clarity, the explicit ordering of layers is given in descriptions of the figures. The letter A stands for metamaterial layer and B for dielectric layer.

Effect of layer thickness. The influence of the thicknesses of layers on transmission and reflection properties is presented in Fig. 7 (in comparison with Fig. 5).

Effect of environment refractive index. Figure 8 presents results for a structure placed in an environment with refractive index not equal to 1. As could be expected,

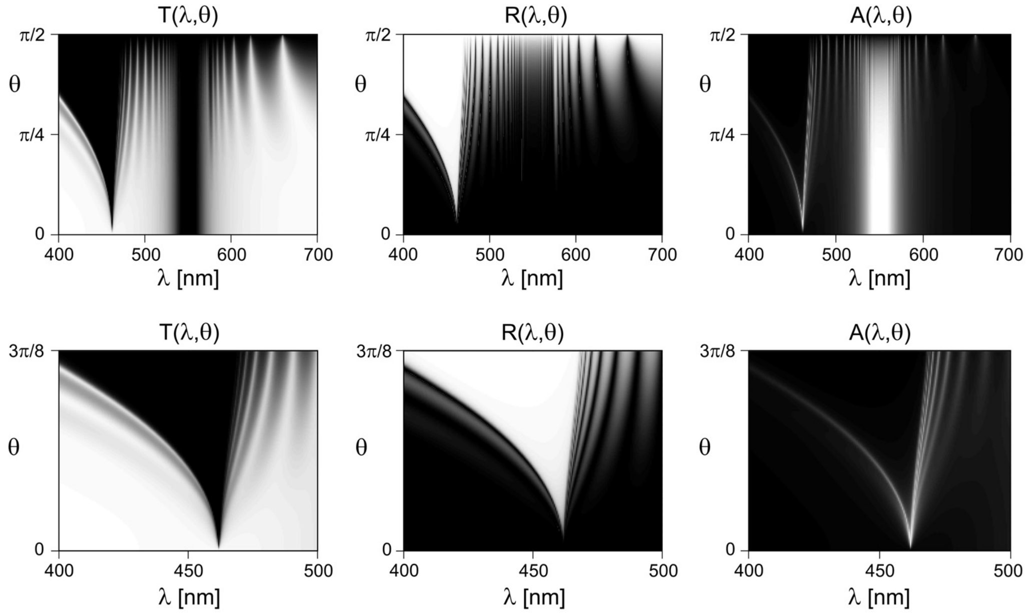

Fig. 6. Top: transmittance, reflectance and absorption for superlattice with ten periods (ABABABABAB-ABABABABAB), placed in air; $d_A = d_B = 40$ nm. Bottom: a fragment of the map, magnified.

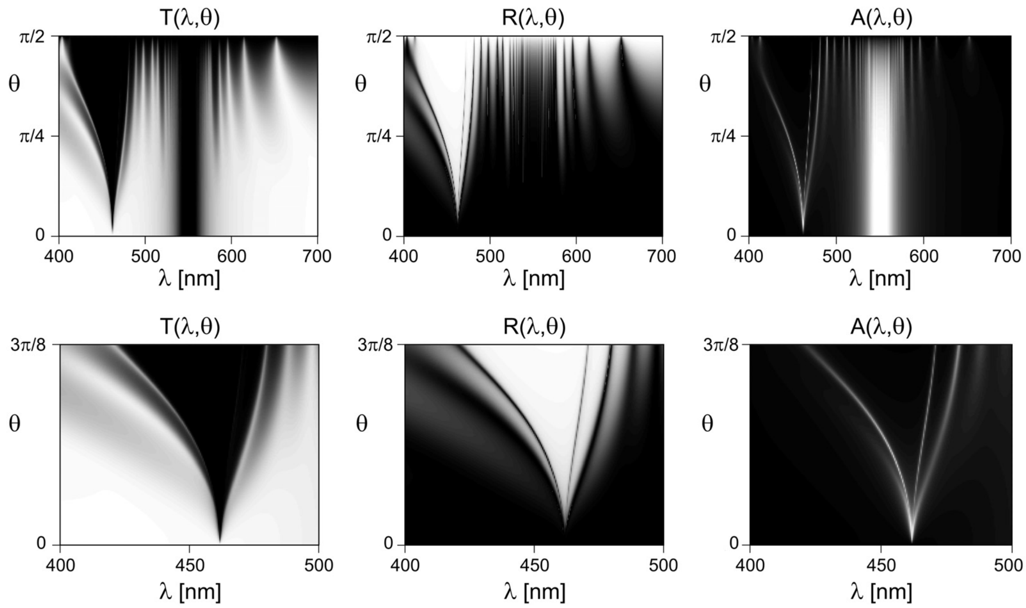

Fig. 7. Top: transmittance, reflectance and absorption for Fibonaccian superlattice (7-th generation, ABAABABAABAABABAABABA), placed in air; $d_A = d_B = 40$ nm. Bottom: a fragment of the map, magnified.

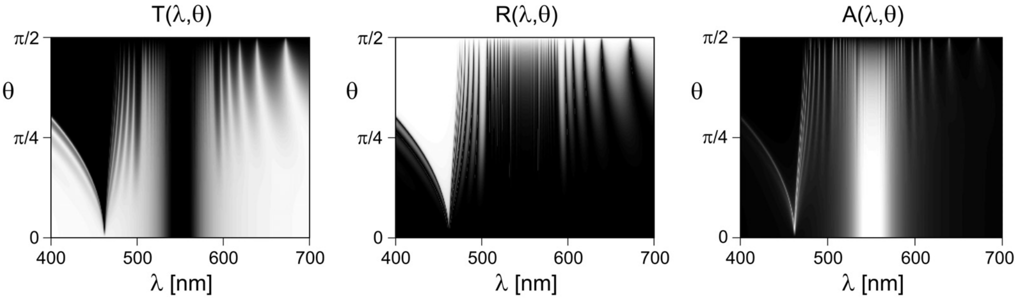

Fig. 8. Transmittance, reflectance and absorption for superlattice with ten periods, placed in air. The thicknesses of A and B layers are different: d_A = 60 nm, d_B = 40 nm.

there occurs total internal reflection on the interface between the external medium and the structure under study for sufficiently large incidence angles. Moreover, low transmission in different wavelength ranges is either due to strong reflection ($\lambda \approx 450$ nm) or to significant absorption ($\lambda \approx 550$ nm).

5. Conclusions and remarks

Based on the results, the following conclusions can be drawn:

1. The phenomenon of total internal reflection occurs for a single LHM layer for the wavelength values, where absolute value of refractive index is lower than one. However, for a sufficiently thin layer, tunnelling appears, which can be seen by comparing Figs. 3 and 4, with details being presented in Fig. 5.
2. In multilayered structures, transmission bands appear inside “V-shaped” total reflection area (Fig. 6), which is an interesting and new result.
3. An increase of metamaterial layer thickness results in an increase of absorption values and by the broadening of absorption bands. Simultaneously, transmission and reflection bands become narrower and more numerous (Figs. 3 and 4).
4. The position of transmission bands depends on layer ordering (Figs. 6 and 7), their thicknesses (Figs. 6 and 8), as well as on the value of the refractive index of the environment. However, describing the character of those dependences qualitatively would demand additional calculations.
5. The unexpected “V-shaped” absorption bands appear on borderlines between transmission and reflection bands (the last maps in Figs. 3, 6 and 7).

Let us discuss briefly the first and the last conclusion. The light tunneling plays a significant role in very thin films (thickness about 50 nm). In the left part of Fig. 3 (thin metamaterial film) there is noticeable transmittance in the wavelength range of 400–500 nm and incidence angle range of 0.16π–0.36π, while transmittance is absent in Fig. 4 (thick metamaterial slab). Moreover, the light tunneling manifests itself by fuzzy borderlines between high transmittance and high reflectance areas in Fig. 3. In Figure 4, analogous borderlines are very sharp, which is the effect of the total

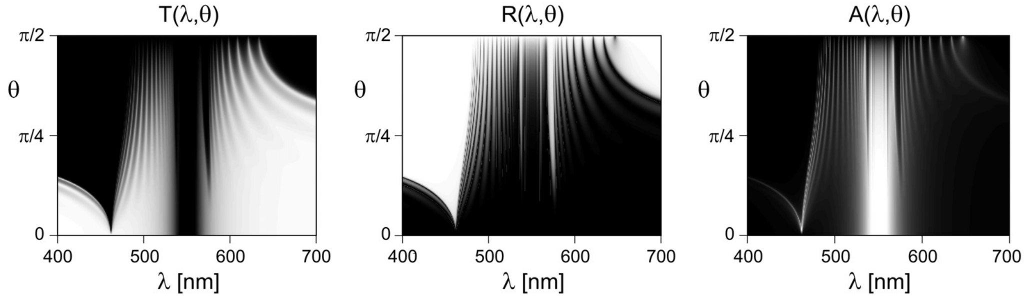

Fig. 9. Transmittance, reflectance and absorption for superlattice with ten periods, placed in an environment with $n_{in} = n_{out} = 2$; $d_A = d_B = 40$ nm.

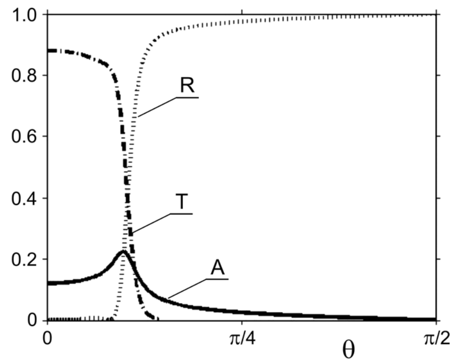

Fig. 10. Cross-section of T, R, A maps, from Fig. 4, $\lambda = 480$ nm.

internal reflection. In order to show this phenomenon, Fig. 9 presents difference in transmittance, between maps from Figs. 3 and 4, in the range of 400–500 nm.

The appearance of "V-shaped" absorption bands, mentioned in point 5, is connected with the absorption in LHM slab and the total internal reflection. The effect of strong absorption is observed on maps for the values of λ and incidence angle θ lying in the immediate neighborhood of the regions of plane (λ, θ) corresponding to the total internal reflection.

We have studied dependences of $T(\lambda, \theta)$, $R(\lambda, \theta)$ and $A(\lambda, \theta)$ for $\lambda = \text{const}$. In Figure 10, we present $T(\lambda, \theta)$, $R(\lambda, \theta)$ and $A(\lambda, \theta)$ for $\lambda = 480$ nm. With decreasing values of incidence angle we observe subsequently:

– total internal reflection for $\theta > \theta_{cr}(\lambda)$,

– for θ close to $\theta_{cr}(\lambda)$ the wave penetrates a single LHM layer and we observe relatively strong absorption,

– when θ comes close to 0 transmission increases to maximum, however, some absorption is still observed and A tends to constant value.

We comment qualitatively this dependence of absorption on incidence angle. Our analysis based on the approach of complex wave vectors [20] allows us to state the following. For normal incidence angle the wave penetrates metamaterial layer and is partially absorbed. With an increase of incidence angle the absorption grows as long

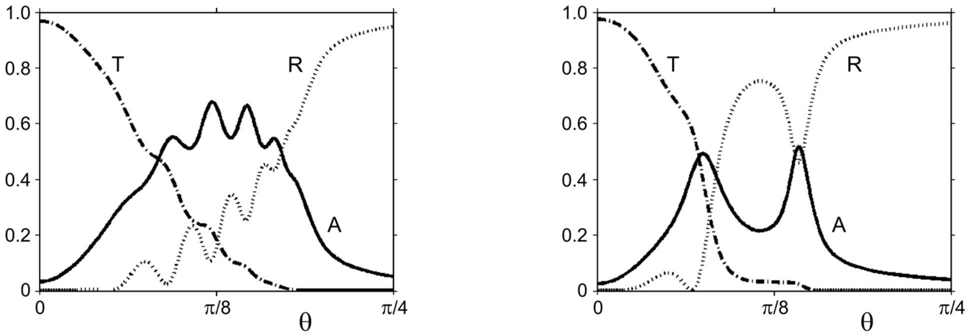

Fig. 11. Cross-sections of *T*, *R*, *A* maps, from Fig. 5 (left) and Fig. 6 (right), $\lambda = 464$ nm.

as $\theta < \theta_{cr}(\lambda)$. Beyond this limit, the total internal reflection does not allow the wave to propagate in metamaterial slab and *A* drops rapidly (Fig. 10).

Similar tendencies can be observed for multilayered structures (Fig. 11). The local maxima of reflectance, connected with constructive interference, coincide with the local minima of absorption.

In this paper we have presented preliminary numerical results, which need further investigation (both numerical and analytical).

Acknowledgements – The work was supported in part by European Network of Excellence for Micro-Optics NEMO. We are grateful to the Referee for valuable and inspiring remarks.

References

[1] FEISE M.W., SHADRIVOV I.V., KIVSHAR Y.S., *Tunable transmission and bistability in left-handed band-gap structures*, Applied Physics Letters **85**(9), 2004, pp. 1451–3.

[2] LIFSHITZ R., ARIE A., BAHABAD A., *Photonic quasicrystals for nonlinear optical frequency conversion*, Physical Review Letters **95**(13), 2005, p. 133901.

[3] MANZANARES-MARTÍNEZ B., RAMOS-MENDIETA F., *Propagation of acoustic waves through finite superlattices: Transmission enhancement by surface resonance assistance*, Physical Review B: Condensed Matter and Materials Physics **66**(9), 2002, p. 092302.

[4] CHAN M.-C., ZHANG Z.-Q., *Lateral transport in quasiperiodically ordered layered media with isotropic randomness*, Waves in Random Media **12**(2), 2002, pp. 201–9.

[5] ZHANG Z.-Q., *Light amplification and localization in randomly layered media with gain*, Physical Review B: Condensed Matter **52**(11), 1995, pp. 7960–4.

[6] BLIOKH K.YU., FREILIKHER V.D., *Localization of transverse waves in randomly layered media at oblique incidence*, Physical Review B: Condensed Matter and Materials Physics **70**(24), 2004, p. 245121.

[7] DONG Y., ZHANG X., *Unusual transmission properties of wave in one-dimensional random system containing left-handed-material*, Physics Letters A **359**(5), 2006, pp. 542–6.

[8] BALUNI V., WILLEMSEN J., *Transmission of acoustic waves in a random layered medium*, Physical Review A: General Physics **31**(5), 1985, pp. 3358–63.

[9] SCALES J.A., VAN VLECK E.S., *Lyapunov exponents and localization in randomly layered media*, Journal of Computational Physics **133**(1), 1997, pp. 27–42.

[10] KLAUZER-KRUSZYNA A., SALEJDA W., TYC M.H., *Polarized light transmission through generalized Fibonacci multilayers. I. Dynamical maps approach*, Optik/Optics **115**(6), 2004, pp. 257–66.

[11] KLAUZER-KRUSZYNA A., SALEJDA W., TYC M.H., *Polarized light transmission through generalized Fibonacci multilayers. II. Numerical results*, Optik/Optics **115**(6), 2004, pp. 267–76.
[12] KLAUZER-KRUSZYNA A., *Propagation polarized light in selected aperiodic superlattices*, PhD Thesis, Wrocław University of Technology, Wrocław 2005 (in Polish).
[13] SALEJDA W., KLAUZER-KRUSZYNA A., TYC M.H., TARNOWSKI K., *Electromagnetic wave propagation through aperiodic superlattices composed of left- and right-handed materials*, SPIE Proceedings Series **5955**, 2005, p. 595514.
[14] SALEJDA W., TYC M.H., KLAUZER-KRUSZYNA A., TARNOWSKI K., *Photonic band structure of the quasi-one-dimensional photonic quasicrystals*, SPIE Proceedings Series **5950**, 2005, p. 59501R.
[15] TARNOWSKI K., SALEJDA W., TYC M.H., KLAUZER-KRUSZYNA A., *Propagation of polarized light through superlattices composed of left- and right-handed materials*, SPIE Proceedings Series **6581**, 2007, p. 658113.
[16] TYC M.H., SALEJDA W., KLAUZER-KRUSZYNA A., TARNOWSKI K., *Photonic band structure of one-dimensional aperiodic superlattices composed of negative refraction metamaterials*, SPIE Proceedings Series **6581**, 2007, p. 658112.
[17] SHELBY R.A., SMITH D.R., SCHULTZ S., *Experimental verification of a negative index of refraction*, Science **292**(5514), 2001, pp. 77–9.
[18] ZIOLKOWSKI R.W., *Pulsed and CW Gaussian beam interactions with double negative metamaterial slabs*, Optics Express **11**(7), 2003, pp. 662–81.
[19] YEH P., *Optical Waves in Layered Media*, Wiley, New York 1988.
[20] SUFFCZYŃSKI M., *The Electrodynamics*, PWN, Warszawa 1980 (in Polish).

Received May 16, 2007
in revised form July 20, 2007